J. Coat. Technol. Res., **19** (3) 977–988, 2022
https://doi.org/10.1007/s11998-021-00577-8

Preparation of PVA/PU/PUA microcapsules and application in self-healing two-component waterborne polyurethane coatings

Xinmeng Xu, Zhongqun Zhou, Liangrong Qin, Caili Yu, Faai Zhang

Received: 31 May 2021 / Revised: 19 October 2021 / Accepted: 24 October 2021

Abstract It is difficult to produce coatings that have good mechanical and self-healing properties. In this study, polyvinyl alcohol/polyurethane/polyurea (PVA/PU/PUA) microcapsules (MCs) loaded with isophorone diisocyanate (IPDI) as core materials were first prepared by interfacial polymerization in an oil-in-water emulsion using different PVA as an emulsifier. The MCs were then uniformly dispersed in the matrix. Optical microscopy and scanning electron microscopy revealed that the size of MCs decreased as alcoholysis and polymerization degree of PVA increased. Thermogravimetric analysis showed that the MCs prepared with the high polymerization or alcoholysis degree of PVA revealed outstanding thermal stability, and the initial decomposition temperature increased by approximately 100°C compared with IPDI. Furthermore, the self-healing performance of the two-component waterborne polyurethane (2K WPU) coating system containing MCs was investigated. The 2K WPU coatings with 9 wt% PVA/PU/PUA MCs exhibited excellent self-healing, mechanical properties, and corrosion resistance, and indicated a high potential for smart coating.

Keywords Microcapsules, PVA/PU/PUA, Self-healing, Two-component waterborne polyurethane, Corrosion resistance

Introduction

Coatings are inevitably damaged during the service process, which significantly reduces the mechanical properties, water and solvent resistance, and other properties of the coating; thus, the substrates cannot be effectively protected.[1–4] Therefore, developing self-healing coatings similar to organisms with dual perception and response function is critical. The self-healing material was first successfully prepared by White et al.[5] It has received much attention because of its potential to extend material life and reduce material maintenance costs.[6,7] Material and energy supply in time are the keys to the self-healing function. Self-healing materials are divided into two types based on their supply method: extrinsic self-healing materials, which are reliant on external repairing agents (e.g., microcapsules (MCs),[8] capillary networks,[9] and hollow glass fibers[10]) to complete self-healing behavior, and intrinsic self-healing materials, which are reliant on reversible covalent bonds/noncovalent bonds to achieve self-healing behavior.[11]

Microencapsulated self-healing materials are the first to be introduced and the most typical extrinsic ones. Self-healing is achieved by rupturing the MC shell, allowing the liquid healing agents to stream out and repair the crack or fracture in the damaged area, thereby extending the service life of the material and saving the high cost of material repair.[12] This technology has become a popular technology for coating repair because of its simple operation, low cost, and high effectiveness. It has huge application prospects in the construction, automotive, and aerospace industries. The core materials of the MCs mainly include dicy-

Supplementary Information The online version contains supplementary material available at https://doi.org/10.1007/s11998-021-00577-8.

X. Xu, Z. Zhou, L. Qin, F. Zhang (✉)
College of Materials Science and Engineering, Guilin University of Technology, No. 12, Jiangan Road, Guilin 541004, People's Republic of China
e-mail: zhangfaai@glut.edu.cn

C. Yu (✉)
College of Chemistry and Biology Engineering, Guilin University of Technology, No. 319, Yanshan Street, Guilin 541006, People's Republic of China
e-mail: yucl916@163.com

clopentadiene,[13] amines,[14] and isocyanates.[15] Because of their easy reactions with moisture, MCs containing liquid isocyanates have emerged as the most attractive catalyst-free self-healing system.[16]

However, the MCs containing isocyanate have limited applications because of their unsatisfactory mechanical performance and permeability. Therefore, researchers have attempted to synthesize a capsule shell with excellent mechanical properties and low permeability (e.g., multilayer shell, hybrid shell, and shell modified by various reagents).[17–20] Song et al.[21] used interfacial and in situ polymerization techniques to synthesize polyurethane/poly(urea-formaldehyde) (PU/PUF) double-shell MCs loaded with IPDI. Attaei[17,20] prepared SiO_2-polyurea (SiO_2-PUA)/PU hybrid shell MCs loaded with IPDI in a W/O emulsion by interfacial polymerization. Polyvinyl alcohol (PVA) is a high molecular weight polymer that is biodegradable, biocompatible, and nontoxic and has strong hydrogen bonds. Due to its good chemical stability, mechanical properties, and excellent film-forming properties, PVA has been widely used in the fields such as fibers, plastics, adhesives, and medicine.[22,23] In addition, Li et al.[24,25] successfully prepared IPDI-loaded PVA-PUA hybrid MCs in an O/W emulsion by interfacial polymerization with PVA as an emulsifier. The method produces MCs with excellent performance and low cost, and the existence of hydroxyl groups on the PVA surface can improve the compatibility between MCs and PU coating. However, the influence of PVA type on MCs has not been reported, and the development of microcapsules coating with good self-healing and mechanical properties has yet to be reported.

Herein, PVA/PUA MCs loaded with IPDI were synthesized by interfacial polymerization in an O/W emulsion using different PVA as an emulsifier. Thermogravimetric analysis, Fourier transform infrared spectroscopy, scanning electron microscopy, and optical microscopy were used to evaluate the quality, structural and micromorphology analysis of MCs. The effects of polymerization degree and alcoholysis degree of PVA on MCs were investigated. Eventually, self-healing performance and corrosion resistance of a two-component waterborne polyurethane (2K WPU) coating containing MCs were evaluated.

Experimental methods and materials

Materials

Isophorone diisocyanate (IPDI, analytically pure (AR)), polymethylene polyphenyl polyisocyanate (PAPI, AR), diethylene triamine (DETA, AR), and polyvinyl alcohol (PVA_{0588}, PVA_{1778}, PVA_{1788}, PVA_{1799}, and PVA_{2488}, AR) were purchased by Aladdin Industrial Corporation. The hydrophilic modified isocyanate XP 2655 (industrial grade), a curing agent, was provided by Shanghai Kaiyin Chemical Co., Ltd. Toluene (AR) was purchased from Xilong Science and Technology Co., Ltd. Acrylate emulsion (theoretical hydroxyl value 100 mg KOH/g, glass transition temperature 15°C) and deionized water were made by our laboratory.[26] All reagents were used without any purification.

Synthesis of PVA solution

Adding 5 g of PVA (PVA_{0588}, PVA_{1778}, PVA_{1788}, PVA_{1799}, and PVA_{2488}) to 95 g of deionized water, the mixture was stirred at 800 rpm for 0.5 h at room temperature, followed by stirring for an additional 3 h at 80°C, and the PVA solution was cooled to room temperature. The differences between these five PVAs are shown in Table S1.

Synthesis of MCs

Scheme 1 shows the MCs preparation flow diagram and related chemical reaction. At first, 60 g of 5 wt% PVA solutions of different types were stirred for 30 min in a 250 mL three-necked bottle at an agitation rate of 800 rpm. Then, the oil phase (the mixture of 4 g PAPI and 12 g IPDI) was slowly poured into the PVA solution while emulsifying for 5 min. The PVA layer was formed at the interface between the aqueous phase and the oil phase due to the formation of intermolecular hydrogen bonds and additional chemical bonds between the –OH groups of PVA (Scheme 1a). During this process, a small amount of isocyanate was incorporated into the PVA layer. Compared with the IPDI monomer, the PAPI monomer has higher reactivity, so PU/PUA_1 in the PVA layer was formed by the reaction of PAPI and PVA/water (Scheme 1b and c). Deionized water (10 mL) was mixed with 0.025, 0.050, 0.100, 0.200, 0.400, or 0.800 g of DETA, respectively, and then sequentially dropped into the PVA emulsion within 1 h. The system was maintained at 65°C for 2 h with a stirring speed of 300 rpm. Interfacial polymerization of DETA and PAPI monomers from the core resulted in the formation of a PUA_2 (Scheme 1d). The MCs were washed with deionized water for at least five times and dried in a glass dish at room temperature for 24 h before further analysis. According to PVA type, MCs are represented by MC_{0588}, MC_{1778}, MC_{1788}, MC_{1799}, and MC_{2488}.

Preparation of self-healing 2K WPU coatings

Firstly, a certain amount of MCs was slowly added to the acrylate emulsion and stirred with a magnetic stirrer until a uniformly dispersed mixture was formed. Then, at an equivalent ratio of 1.2, curing agent XP 2655 was added to the above mixture and stirred for 3 min. Finally, the mixture was coated on a tinplate and glass plate with a linear coater, dried for 24 h at room

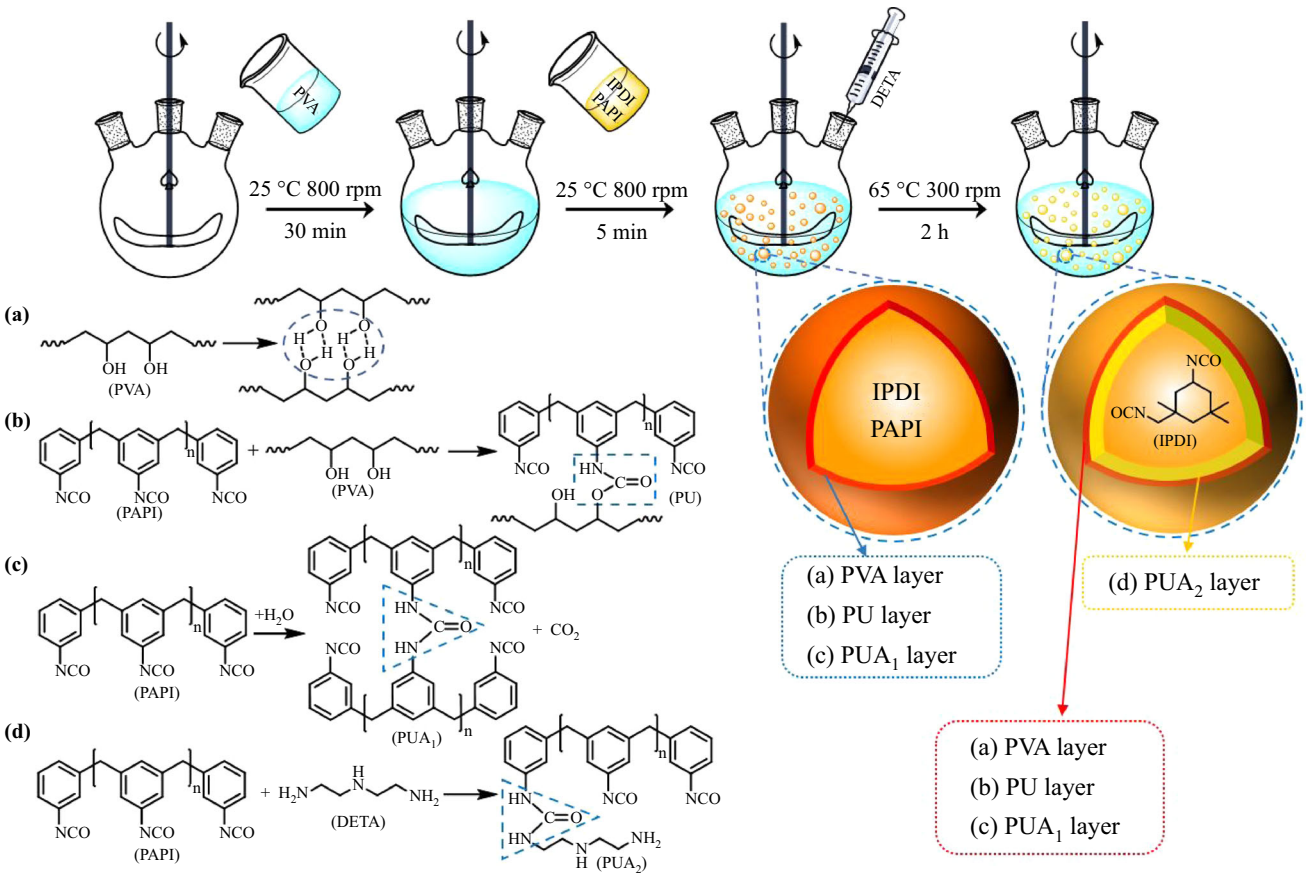

Scheme 1: The preparation flow diagram and related chemical reaction of MCs

temperature, and then dried at 60°C for 24 h to obtain a coating film. According to MC type, 2K WPU is represented by 2K WPU_{0588}, 2K WPU_{1778}, 2K WPU_{1788}, 2K WPU_{1799}, and 2K WPU_{2488}.

Characterization

The infrared spectroscopy of samples was recorded by Thermo Nexus 470 Fourier transform infrared (FTIR) spectrometer. The liquid sample was evenly coated on potassium bromide and then tested after being dried under an infrared lamp. The powder sample was mixed with the potassium bromide and pressed. The measurement range was 4000 ~ 400 cm^{-1}. The morphology, size distribution, average shell thickness, and self-healing effect of MCs were observed by S-4800 field emission scanning electron microscope (FESEM, Japan High-tech Company) under 5 ~ 10 kV voltage. Samples were pre-coated with conductive Au films by sputtering using Q150T ES sputtering coater (Quorum Technologies). Thermogravimetric analysis (TGA) measurements were conducted using a TA Instruments analyzer (TGA Q500, USA) in N_2. The samples were ramped from RT to 800°C at a heating rate of 10°C min^{-1}. MCs and coatings were observed and photographed by Leica DM P×P optical microscope (OM, Germany Leitz Company) to evaluate the shell maturity, and size of MCs and the distribution of MCs in coatings during synthesis. The thermal stability of the samples was tested by an American TA-209 thermogravimetric analyzer in an N_2 atmosphere. The measuring range was 30 ~ 800°C, and the heating rate was 10 K/min. Saline immersion method was used to evaluate the corrosion resistance of the coatings. Firstly, a crossing scratch was made on the coating surface with the same manner, where all scratched samples were left for 48 h to allow for healing and then immersed in 3.5 wt% NaCl solution, and a camera was used to record the corrosion state of coatings in different immersion time. Electrochemical impedance spectroscopy (EIS) was carried out by using an electrochemical workstation (CHI 760E, Shanghai Chenhua Instrument Co., Ltd. China) in a three-electrode system. The EIS measurements were performed in a 3.5 wt% NaCl solution with a frequency range from 10^5 Hz to 10^{-2} Hz and an amplitude of 5 mV. The mechanical performance was tested by the UTM4503SLXY universal tensile testing machine from Shenzhen Sansi aspect Technology Co., Ltd., with 50 mm/min tensile rate, and Young's modulus, breaking strain, and tensile stress were obtained by mechanical performance test. The pendulum hardness, impact resistance, and gloss were tested according to GB/T

1730-2007, GB/T 1732-1993, and GB/T 1743-1979 methods, respectively. Adhesion test was adopted to BGD 501 automatic circling method by adhesion tester, and the results referred to GB/T 1720-79.

The core content (η) of MCs obtained by TGA was calculated by equation (1):

$$\eta = 1 - R_{MCs}/R_{shell} \times 100\% \quad (1)$$

where R_{MCs} and R_{shell} are the residue ratios of MCs and shell at 800°C, respectively.

Results and discussion

Analysis and characterization of MCs

FTIR

Figure S1 shows the spectra of each component of the prepared MCs. Compared with the PAPI spectra, the characteristic absorption peak at 2259 cm^{-1} attributed to the isocyanate group (–NCO) in the shell is reduced significantly. The characteristic absorption peaks near 3358 and 1645 cm^{-1} that correspond to N–H and C=O of PUA, and the characteristic peaks at 1600 and 1510 cm^{-1} that correspond to the C–C stretching vibration in the benzene ring, existed, indicating that –NCO in PAPI reacted with DETA or water to form a PUA shell. The complete MCs show a very strong –NCO absorption peak at 2259 cm^{-1}, indicating that IPDI has been successfully coated on the basis of nearly similar spectra for pure IPDI and the core.

Morphology

OM and FESEM were used to evaluate the morphology, size distribution, and shell thickness of the MCs. The morphologies of MCs during the preparation of MC_{1788} were observed by OM and are shown in Fig. S2. Relatively stable MCs produced after the emulsification process were completed (Fig. S2a), which may be caused by PVA tending to form interconnected networks at the interface between the water and oil phases through hydrogen bonds, and the isocyanates reacted with the hydroxyl group of the PVA to form PU during emulsification. The color of MCs became dark with the addition of DETA (Fig. S2b and c), indicating that the thickness and crosslinking density of the MCs shell layer increased with the increase in reaction time. In addition, wrinkles existed on the surface of MCs, which were mainly due to the highly crosslinked shell resisting the liquid core's shrinkage.

The effects of different PVA on the size of MCs were observed via OM (Fig. 1). The polymerization and alcoholysis degrees of PVA exert a significant impact on the particle size of the MCs. The average diameter of the MCs decreased from 39 to 20 μm as the PVA molecular weight increased from 22,000 (PVA_{0588}) to 105,600 (PVA_{2488}) at the alcoholysis degree of 88%, whereas the average diameter of the MCs decreased from 36 to 25 μm as the PVA alcoholysis degree increased from 78% (PVA_{1778}) to 99% (PVA_{1799}) at the molecular weight of 74,800. This is because the viscosity of PVA increases with the increase in polymerization degree or alcoholysis degree of PVA, decreases the surface tension, and leads to small particle size of MCs.[27,28]

Figure 2 shows the surface and shell morphology of MCs. The MCs prepared with PVA as an emulsifier were optically transparent and dispersed individually without adhering to each other. The outer and inner surfaces of the capsules were smooth, and the shell wall thickness was roughly uniform at 2 μm. The polymerization and alcoholysis degrees of PVA have little effect on the surface morphology and shell thickness of MCs.

TGA thermal analysis

The thermal properties of MCs and core material were investigated using TGA thermal analysis. The decomposition of MCs was divided into three stages (Fig. 3a). The first stage was mainly due to IPDI (liquid core), and the last two stages were due to the shell. The initial decomposition temperature ($T_{5\%}$) of the IPDI monomer was 130°C, and it was nearly completely lost at 228°C. However, IPDI encapsulated in MCs demonstrated remarkable thermal stability ($T_{5\%}$ > 186°C). This reinforcement can be attributed to the double barrier from PUA and PVA. Among them, MC_{1799} and MC_{2488} showed high thermal stability. This is mainly due to a high polymerization and alcoholysis degrees of PVA, which make MCs with denser shells through enhanced entanglement effect associated with hydrogen bonds between intermolecular and interchains, as well as microcrystallization, resulting in higher thermal stabilities.[29,30] Figure 3c shows that the residual weights of MCs and pure IPDI vary with time during the isothermal process of 100 min at 100°C. By comparison, pure IPDI loses approximately 43.6 wt% of the original sample, whereas the encapsulated IPDI loses approximately 0.5 wt% after the same process. This means that the encapsulated IPDI had a slower evaporation rate, and it also confirmed that the resulting shells have better thermal resistance than pure IPDI.

Table 1 shows the core contents of MCs. TGA curves also showed that IPDI was encapsulated in the MCs with a mass ratio of approximately 59–68 wt%. In addition, the η values of MC_{0588}, MC_{1778}, and MC_{1788} (66.6, 68.0, and 65.3 wt%, respectively) were higher than those of MC_{1799} and MC_{2488} (61.6 and 59.0 wt%, respectively). This confirmed the finding that the core content was related to MCs size and surface wrinkles,

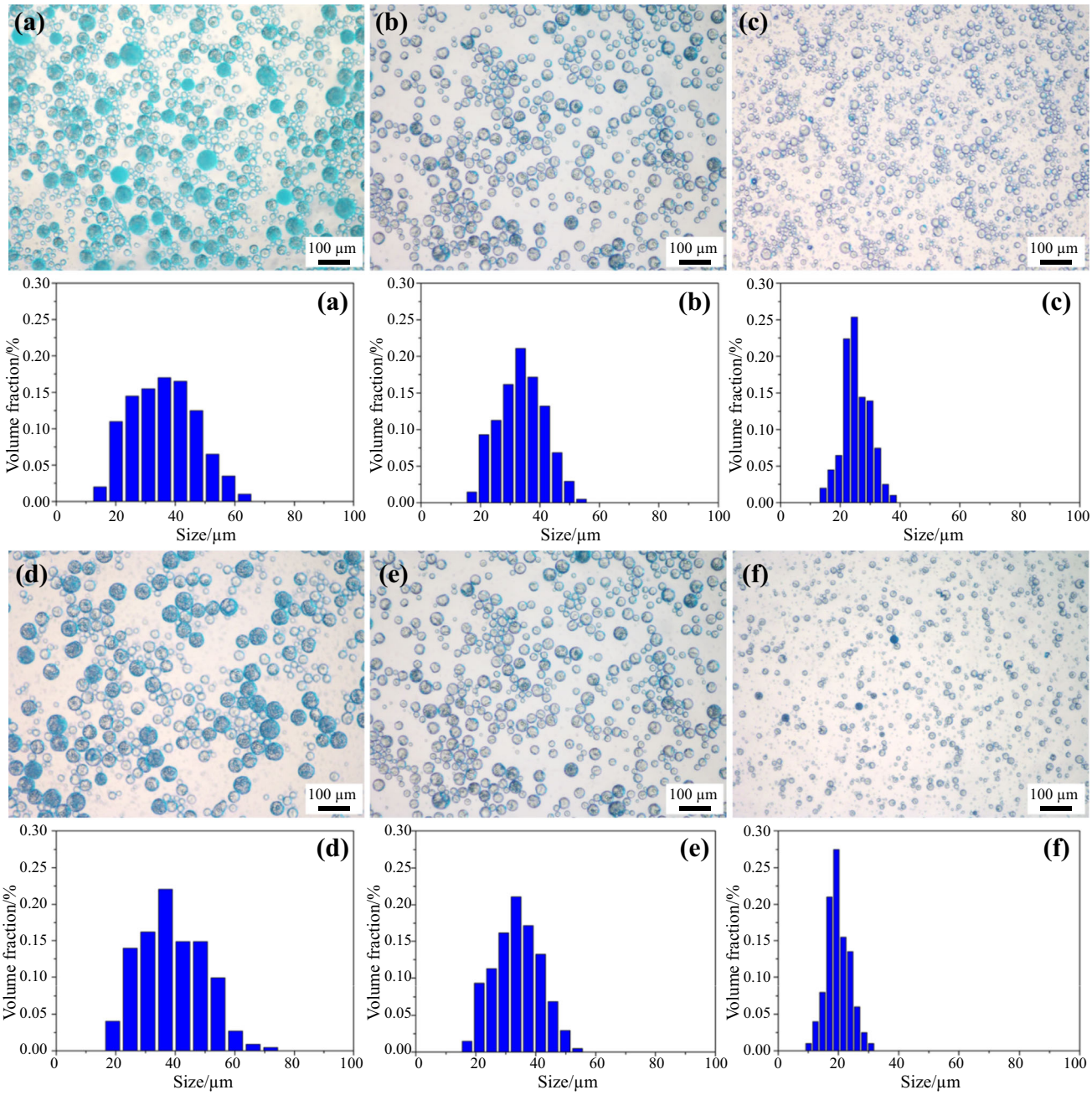

Fig. 1: OM images and particle size distribution of MC_{1778} (a), MC_{1788} (b), MC_{1799} (c), MC_{0588} (d), and MC_{2488} (e)

and that the MCs with high core content had larger sizes and fewer surface wrinkles.

To further investigate the stability of the IPDI-loaded MCs in a wet environment, an aqueous solution-immersion experiment was conducted, and the core contents of MCs were analyzed using TGA. As shown in the TGA traces in Fig. S3, the core contents of MCs gradually decrease with the immersion time. More than 45 wt% of the active reagents were retained in the core because of the dense shell layer prohibiting water from penetration after 7 days of immersion. The core contents of MC_{0588}, MC_{1778}, MC_{1788}, MC_{1799}, and MC_{2488} were reduced by 26.7, 28.8, 26.5, 23.9, and 24.2 wt%, respectively. Among them, MC_{1799} and MC_{2488} encapsulated less amount of IPDI; however, they showed the least decline. This shows that PVA with a high polymerization and alcoholysis degrees result in the MCs with lower permeability, implying that the active agent can be effectively protected. Furthermore, the decreased core content may be due to the reaction between diffused water across the shell and the encapsulated active core IPDI, which was further proved by the SEM images of the core morphology of MCs after soaking in water. The MCs nearly turned

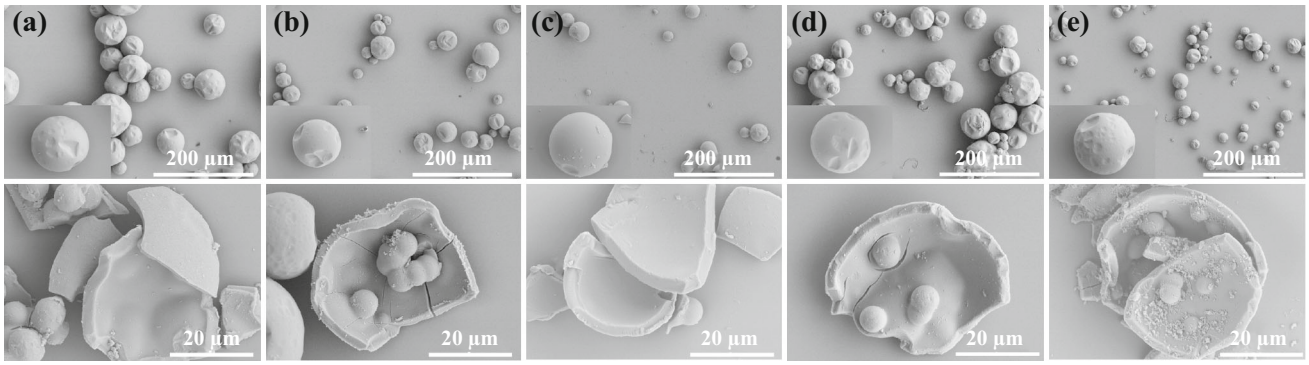

Fig. 2: SEM images of MCs (upper) and MCs shells (lower) prepared with PVA_{1778} (a),PVA_{1788} (b), PVA_{1799} (c), PVA_{0588} (d), and PVA_{2488} (e) as emulsifiers

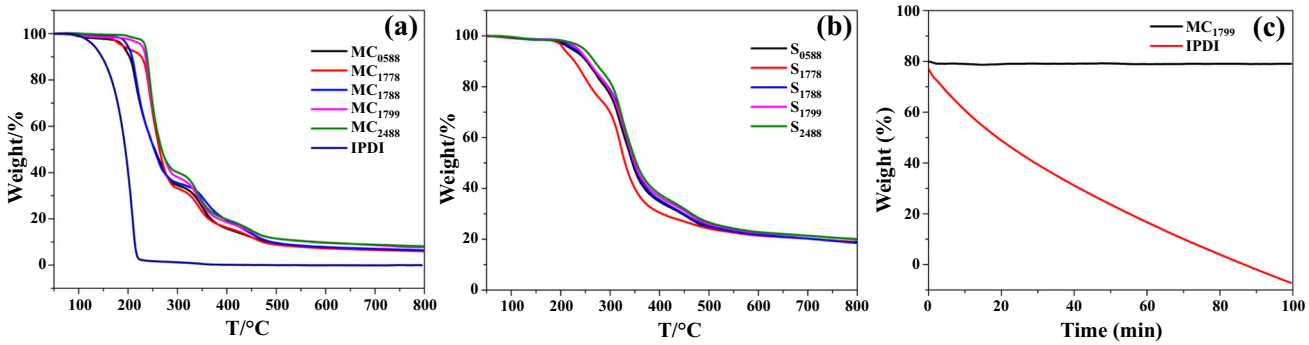

Fig. 3: TGA of IPDI, MCs, and shells (a) TGA of IPDI and MCs, (b) TGA of MC shells, (c) TGA of MC_{1799} and IPDI at 100°C

Table 1: Thermal weight loss data of MCs and capsule shells

PVA type	T5%(MCs) /°C	T5%(shell) /°C	Residual (MCs) /%	Residual (shell) /%	η /wt%
0588	188	220	6.32	18.91	66.6
1778	186	205	5.97	18.65	68.0
1788	198	226	6.43	18.55	65.3
1799	226	234	7.71	20.11	61.6
2488	234	245	8.16	19.92	59.0

into solid particles (Fig. 4b), which show that water molecules passed through the capsule wall and reacted with IPDI to form PUA during the soaking process of MCs, and indirectly proved the self-healing performance of MCs.

Self-healing performance of 2K WPU

OM analysis

OM was used to observe the coatings containing 15 wt% MCs to evaluate the distribution of MCs in the 2K WPU the coatings. The large-sized MCs (MC_{0588}, MC_{1778}, and MC_{1788}) are broken because they cannot withstand the shear stress generated during the high-speed stirring process (Fig. 5).[31] However, the MC_{1799} and MC_{2488} have almost no fragmentation and are evenly distributed in the coatings. This is mainly due to the shear stress; the larger the MCs, the greater the stress exerted, and the easier it is to be ruptured.

In addition, the mechanical properties of the various pure PVA coating film can account for this result. The representative tensile curves of different PVA coating films are shown in Fig. S4. The tensile strength and Young's modulus of the PVA coatings increased as the molecular weight or alcoholysis degree increased. At a 50 mm/min strain rate, the Young's modulus and tensile strength of PVA_{1799} are 208 and 25 MPa, respectively, whereas the Young's modulus and tensile strength of PVA_{2488} are 128 and 32 MPa, respectively. The Young's modulus and tensile strength of the

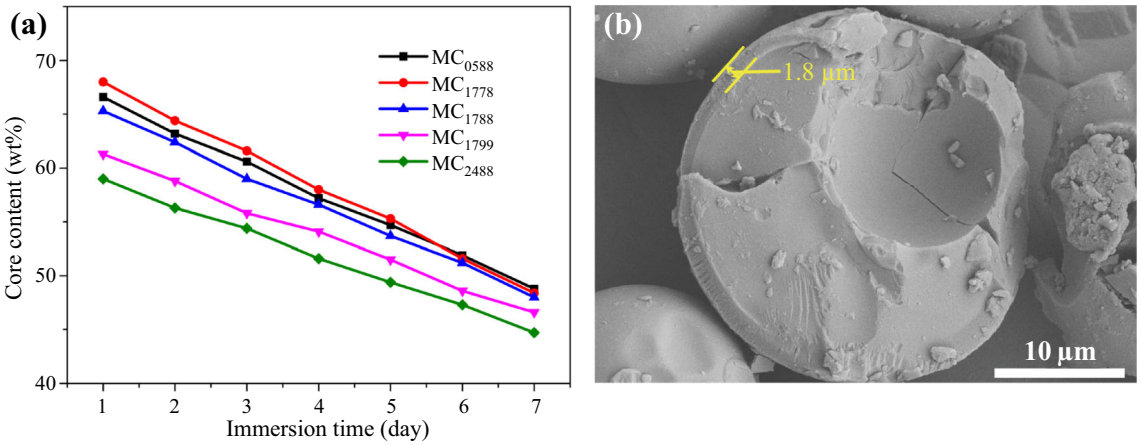

Fig. 4: Core contents of the MCs after immersion in water for different time (a) and SEM images of MCs after 30 d soaking (b)

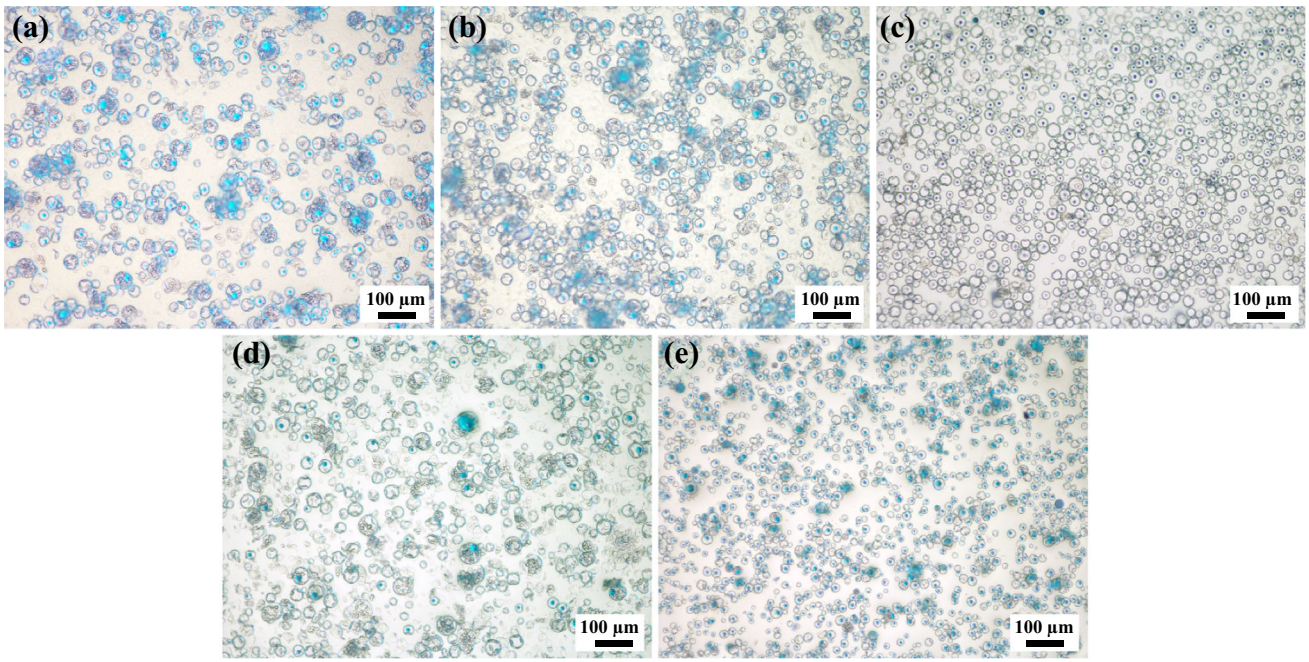

Fig. 5: OM images of 2K WPU coatings with 15 wt% MC_{1778} (a), MC_{1788} (b), MC_{1799} (c), MC_{0588} (d), MC_{2488} (e)

PVA_{1799} and PVA_{2488} coatings films are higher than that of PVA_{0588}, PVA_{1778}, and PVA_{1788} coatings films. PVA_{1788} has the lowest modulus because the number of hydrophilic hydroxyl groups in PVA molecules decreases with the decrease in alcoholysis degree; the ability of PVA molecules to form hydrogen bonds decreases correspondingly, reducing the crystallinity of PVA. The low number of hydrogen bonds and crystallinity of PVA_{1778} lead to its low modulus.

Corrosion protection of self-healing 2K WPU

The as-prepared MCs were dispersed in the acrylate emulsion at a concentration of 15 wt% and then mixed with the curing agent, resulting in 2K WPU coatings that were applied and compared with pure 2K WPU coatings. Both the control and self-healing coating specimens were scratched by artificial penetration with a razor blade. Anticorrosion tests were conducted under accelerated corrosion conditions (immersed in 3.5% NaCl aqueous solution), and the results are shown in Fig. 6. After exposure to the 3.5% NaCl solution for 24 h, visible rust corrosion appeared in the scratched regions of the control specimen. Because of the direct exposure to the corrosive solutions, severe corrosion and further expansion of corrosion near the scratched area of the control specimen were observed over time to 48 h. However, the 2K WPU coatings incorporated with the MCs exhibited excellent corro-

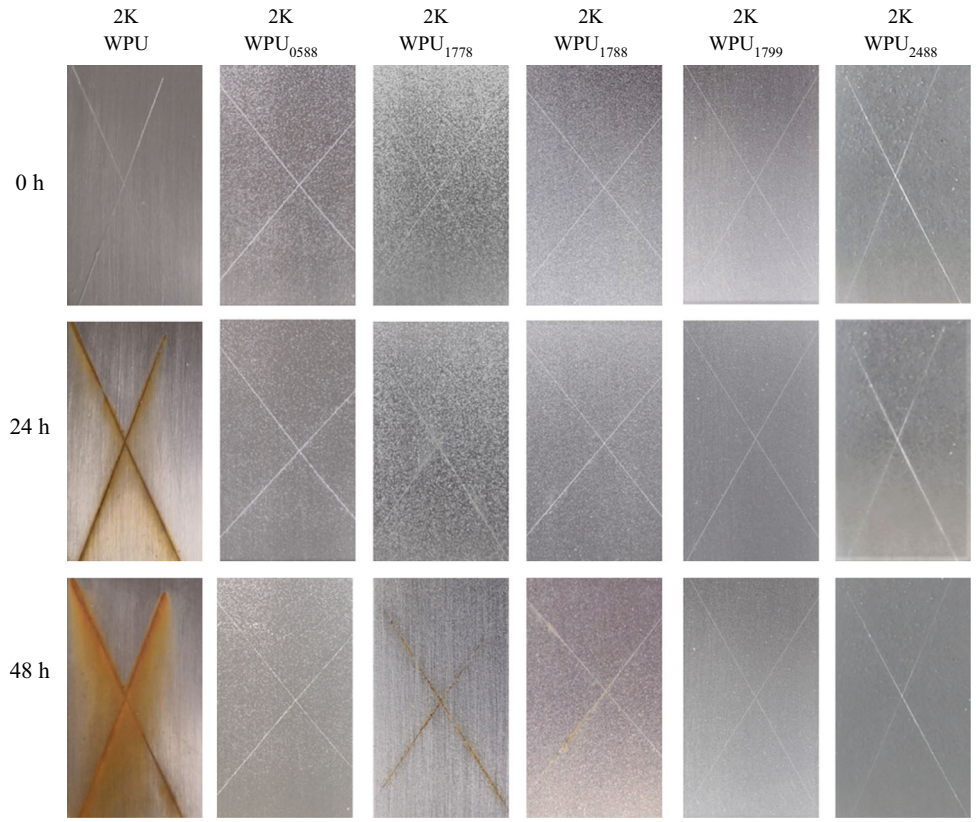

Fig. 6: Photographs of tinplate coated with neat 2K WPU and 2K WPU coatings incorporated with different types of MCs after saline immersion test for different times. MCs content: 15 wt%

Table 2: Film performance of 2K WPU coatings loaded with different types of MCs

2K WPU types	2K WPU	2K WPU_{0588}	2K WPU_{1778}	2K WPU_{1788}	2K WPU_{1799}	2K WPU_{2488}
Impact strength (positive/reverse)/kg·cm	50/50	25/20	15/20	25/20	50/35	50/35
Glossiness	150±0.7	71±4.1	62±4.7	75±3.6	88±2.0	90±1.8
Adhesion/level	2	4	4	4	3	3
Pendulum hardness, s	298	317	314	315	312	309
Flexibility/mm	1	2	3	2	1	1

MCs content: 15 wt%

sion inhibition, especially the 2K WPU_{1799} and WPU_{2488} coatings. The outstanding anticorrosion performances of the self-healing coating on tinplate are attributed to the fact that the released IPDI from MCs formed a new barrier layer in the damaged area after reaction with water. Different degrees of corrosion appeared in the scratched regions of the 2K WPU_{0588}, WPU_{1778}, and WPU_{1788} coatings. The larger size MCs were broken because they could not withstand the shear stress generated using the high-speed mixing process, and the broken MCs had no self-healing abilities.

Table 2 shows the film performance of the neat 2K WPU and self-healing 2K WPU coatings. The addition of 15 wt% MCs increased the coating's hardness but reduced the coating's impact strength, adhesion, and flexibility. Especially for MC_{1778}, the impact strength of the coating reduced to 15/20 kg·cm, the adhesion to grade 4, the flexibility to 3 mm, and the glossiness to 62. This is because some MCs may have been broken during the coating preparation process, resulting in the outflow of the core material and subsequent reaction with water to form PUA. This result can be attributed to PUA's high hardness and low toughness. Additionally, as the size of the MCs increased, the gloss of the coatings decreased due to the size of the MCs exceeding the thickness of the coatings. Because the MCs were partially exposed on the surface of the coatings, the coatings were not smooth, resulting in a declined gloss of the coatings. Although the perfor-

mance of WPU_{1799} and WPU_{2488} coatings decreased compared with that of the blank sample, the impact was relatively small. MC_{1799} was selected for subsequent research based on its self-healing performance, coating properties, and cost.

To further prepare coatings with a good film and self-healing properties, a saline immersion test was conducted on 2K WPU coatings with different MC contents, and the results are illustrated in Fig. 7. After 24 h, the rusting process was visible in the coatings containing 3 wt% MCs. However, no sign of rusting or corrosion were visible for samples containing 9, 12, or 15 wt% MCs, even after 48 h of exposure to 3.5% NaCl solution. The results reveal that the enhancement in anticorrosion performance is obvious by increasing the MCs content. The higher MC content led to a higher amount of released healing agents into the scratch area, which effectively improved the barrier performance of the scratch area and the corrosion resistance of the coatings.

Table 3 shows the coating performance of 2K WPU in addition to its self-healing performance. The impact strength, adhesion resistance, and gloss of the coating decreased as the MCs content increases. When the MCs content was reduced to 12 wt%, the adhesion was equivalent to that of the blank one. When it was 6 wt%, the impact strength reached 50/50 kg·cm, but the self-healing performance was not good. Considering comprehensively, the 2K WPU with 9 wt% MCs not only maintained the coating performance of pure 2K WPU, but also endowed the coating with excellent self-healing properties.

Evaluation of self-healing performance by SEM

To investigate the self-healing properties of MC-embedded films, 2K WPU samples with and without MCs were prepared as described in the experimental section. A scalpel blade was used to create an artificial crack on the surface of the sample, and then, the scratched samples were placed at ambient temperature and humidity of 50%–70% for 48 h. The SEM images of the cracked area on the blank or 2K WPU coating with 9 wt% MCs are shown in Figs. 8a and b. Healing was not observed in the blank WPU coating, whereas the MC-embedded 2K WPU coating was nearly completely healed, indicating that MCs-contained 2K WPU coating has good self-healing properties. This is because cracks on the coating surface resulted in the rupture of a larger number of MCs.[32] The released healing agent (IPDI) diffused to the damaged area under the action of siphon and reacted with water in the air, filling the cracks accordingly. This demonstrated that IPDI is an efficient core material for self-

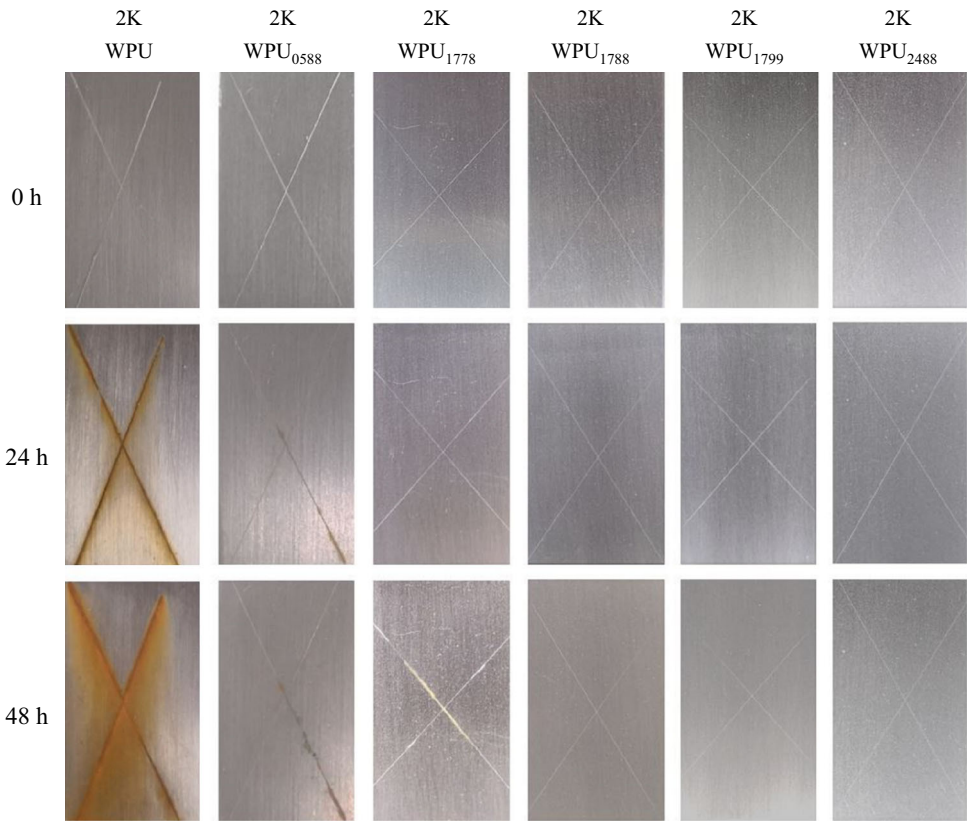

Fig. 7: Photographs of tinplate coated with neat 2K WPU and 2K WPU coatings incorporated with different MCs content after saline immersion test for different times. Conditions: PVA_{1799} as an emulsifier for preparing MCs

Table 3: Coating performance of 2K WPU with different MCs content

MCs content /wt%	0	3	6	9	12	15
Impact strength (positive/reverse)/kg·cm	50/50	50/50	50/50	50/45	50/40	50/35
Adhesion/level	2	2	2	2	2	3
Glossiness (60°)	150±0.7	121±2.7	116±2.3	110±2.5	97±1.9	88±2.0
Pendulum hardness, s	298	299	304	307	313	312
Flexibility/mm	1	1	1	1	1	1

PVA_{1799} as an emulsifier to prepare MCs

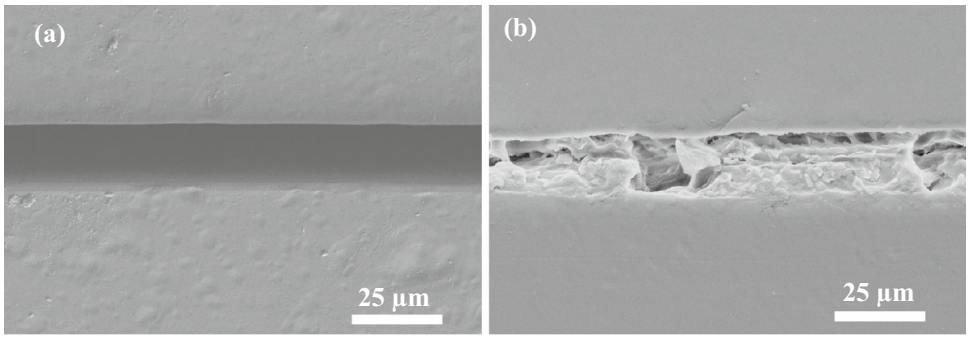

Fig. 8: SEM images of blank 2K WPU coating (a) and the 2K WPU coating (9 wt% MC_{1799}) (b)

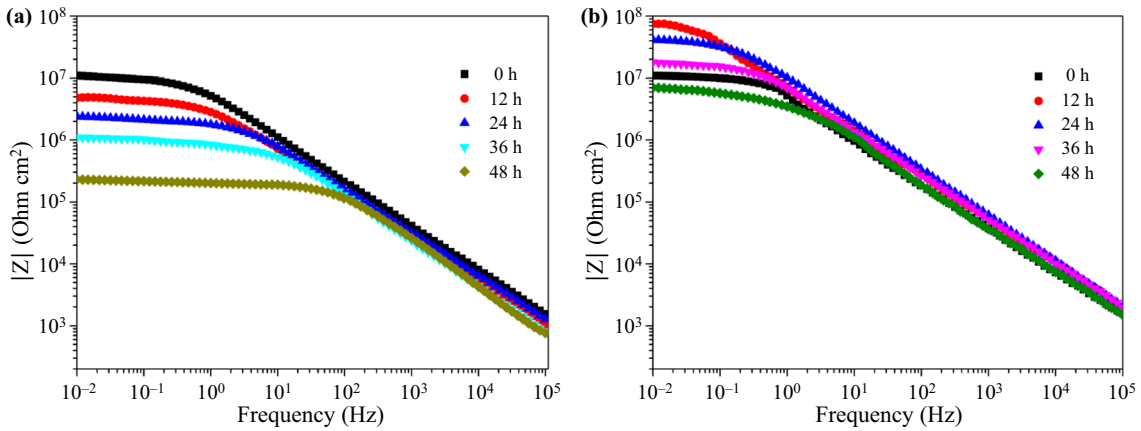

Fig. 9: EIS results of the pure 2K WPU (a) and self-healing coating (b) soaked in 3.5% NaCl solution for different time (self-healing coating with 9 wt% MC_{1799})

healing in a 2K WPU matrix, with a sample containing 9 wt% MC_{1799} being repaired in 48 h.

Evaluation of 2K WPU coatings by EIS

EIS measurements can be used to monitor the self-healing process of damaged areas in 2K WPU coatings.[33] Artificial scratches penetrating the coating were applied on the blank and self-healing coating films and then immersed in 3.5 wt% NaCl aqueous solution for 0, 12, 24, 36, and 48 h before the EIS test. Figure 9 shows the Bode plot for the impedance response of the tinplate substrate coated with blank and self-healing coatings. The |Z| value of scratched pure 2K WPU displays a significant impedance drop (from 1.10×10^7 to 2.29×10^5 at 10^{-2} Hz) with the prolongation of corrosion time, which is due to water and ions penetrating the scratched coating layer. This implies that once microcracks are formed, the pure 2K WPU coating will lose its anticorrosive properties. However, the |Z| value of the scratched self-healing coating with MCs shows a slight increase after immersion for 12 h (from 1.09×10^7 to 7.51×10^7 at 10^{-2} Hz), and it is still significantly higher (7.04×10^6) than that of the blank coatings (2.29×10^5) after immersion for 48 h. It has also demonstrated that the MCs can endow 2K WPU coating with certain self-healing performance, and the

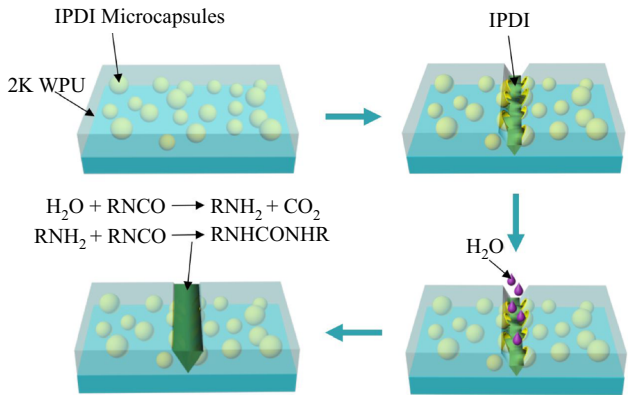

Scheme 2: Schematic diagram of MCs self-healing mechanism

newly formed PUA shows relatively high corrosion resistance by preventing water from entering the tinplate substrate.

Scheme 2 shows a schematic of MCs' self-repair mechanism. When cracks appear in the self-healing 2K WPU coating, they pierce the MCs, releasing the IPDI healing agent, which then reacts with water to form an amine and carbon dioxide, and the amine then reacts with isocyanate to form PUA, producing a new protective barrier on the metal surface. The barrier can effectively reduce metal substrate corrosion at the crack, or inhibit the corrosion spread around the crack, demonstrating a good self-healing and anticorrosion function.

Conclusions

PVA-mediated interfacial polymerization in an oil-in-water emulsion was used to synthesize MCs with IPDI as the core. The size of MCs decreased as the polymerization and alcoholysis degree of PVA increased, and the thermal stability increased with the increase of polymerization and alcoholysis degree of PVA. The highly crosslinked composite capsule shell provided excellent storage stability to MCs. The obtained MCs exhibited excellent compatibility with 2K WPU paint. The film properties of the 2K WPU coating decreased as MCs' size and content increased. The 2K WPU self-healing coating containing 9 wt% MC_{1799} showed excellent self-healing and corrosion resistance while maintaining good film properties. The MCs are widely used in the field of metal corrosion, providing attractive prospective applications in self-healing coatings.

Acknowledgments This work was supported by the National Natural Science Foundation of China (No. 21664005, 51863007); and the Guangxi Program for Hundred Talents for Returned Scholars.

Conflict of interest The authors declare that they have no known competing financial interests or personal relationships that could have appeared to influence the work reported in this paper.

References

1. Syrett, JA, Becer, CR, Haddleton, DM, "Self-Healing and Self-Mendable Polymers." *Polym. Chem.*, **1** (7) 978–987 (2010)
2. Wu, DY, Meure, S, Solomon, D, "Self-Healing Polymeric Materials: A Review of Recent Developments." *Prog. Polym. Sci.*, **33** (5) 479–522 (2008)
3. Trask, RS, Williams, HR, Bond, IP, "Self-Healing Polymer Composites: Mimicking Nature to Enhance Performance." *Bioinspir. Biomim.*, **2** (1) P1–P9 (2007)
4. Hatami Boura, S, Peikari, M, Ashrafi, A, Samadzadeh, M, "Self-Healing Ability and Adhesion Strength of Capsule Embedded Coatings—Micro and Nano Sized Capsules Containing Linseed Oil." *Prog. Org. Coat.*, **75** (4) 292–300 (2012)
5. White, SR, Sottos, NR, Geubelle, PH, Moore, JS, Kessler, MR, Sriram, SR, Brown, E, Viswanathan, S, "Autonomic Healing of Polymer Composites." *Nature*, **409** (6822) 794–797 (2001)
6. Sinha-Ray, S, Pelot, DD, Zhou, ZP, Rahman, A, Wu, XF, Yarin, AL, "Encapsulation of Self-Healing Materials by Coelectrospinning, Emulsion Electrospinning, Solution Blowing and Intercalation." *J. Mater. Chem.*, **22** (18) 9138–9146 (2012)
7. Zhu, DY, Rong, MZ, Zhang, MQ, "Self-Healing Polymeric Materials Based on Microencapsulated Healing Agents: From Design to Preparation." *Prog. Polym. Sci.*, **49–50** 175–220 (2015)
8. Sun, D, Chong, YB, Chen, K, Yang, J, "Chemically and Thermally Stable Isocyanate Microcapsules Having Good Self-Healing and Self-Lubricating Performances." *Chem. Eng. J.*, **346** 289–297 (2018)
9. Vahedi, V, Pasbakhsh, P, Piao, CS, Seng, CE, "A Facile Method for Preparation of Self-Healing Epoxy Composites: Using Electrospun Nanofibers as Microchannels." *J. Mater. Chem. A.*, **3** (31) 16005–16012 (2015)
10. He, Y, Liao, S, Jia, H, Cao, Y, Wang, Z, Wang, Y, "A Self-Healing Electronic Sensor Based on Thermal-Sensitive Fluids." *Adv. Mater.*, **27** (31) 4622–4627 (2015)
11. Alizadegan, F, Mirabedini, SM, Pazokifard, S, Goharshenas Moghadam, S, Farnood, R, "Improving Self-Healing Performance of Polyurethane Coatings Using PU Microcapsules Containing Bulky-IPDI-BA and Nano-Clay." *Prog. Org. Coat.*, **123** 350–361 (2018)
12. Zhang, H, Wang, P, Yang, J, "Self-Healing Epoxy via Epoxy-Amine Chemistry in Dual Hollow Glass Bubbles." *Compos. Sci. Technol.*, **94** 23–29 (2014)
13. Brown, EN, Kessler, MR, Sottos, NR, White, SR, "In Situ Poly(Urea-Formaldehyde) Microencapsulation of Dicyclopentadiene." *J. Microencapsul.*, **20** (6) 719–730 (2003)
14. Yi, H, Deng, Y, Wang, C, "Pickering Emulsion-Based Fabrication of Epoxy and Amine Microcapsules for Dual Core Self-Healing Coating." *Compos. Sci. Technol.*, **133** 51–59 (2016)
15. Ma, Y, Lv, S, Yao, X, Zhang, Y, Gu, J, "Preparation of Isocyanate Microcapsules as a High-Performance Adhesive For PLA/WF." *Constr. Build. Mater.*, **260** 120483 (2020)
16. Li, CM, Tan, JJ, Gu, JW, Qiao, L, Zhang, BL, Zhang, QY, "Rapid and Efficient Synthesis of Isocyanate Microcapsules

via Thiol-ene Photopolymerization in Pickering Emulsion and Its Application in Self-Healing Coating.'' *Compos. Sci. Technol.*, **123** 250–258 (2016)
17. Attaei, M, Vale, M, Shakoor, A, Kahraman, R, Montemor, MF, Marques, AC, ''Hybrid Shell Microcapsules Containing Isophorone Diisocyanate with High Thermal and Chemical Stability for Autonomous Self-Healing of Epoxy Coatings.'' *J. Appl. Polym. Sci.*, **137** (22) 48751 (2020)
18. Sun, D, An, J, Wu, G, Yang, J, ''Double-Layered Reactive Microcapsules with Excellent Thermal and Non-Polar Solvent Resistance for Self-Healing Coatings.'' *J. Mater. Chem. A.*, **3** (8) 4435–4444 (2015)
19. Chen, S, Han, T, Zhao, Y, Luo, W, Zhang, Z, Su, H, Tang, BZ, Yang, J, ''A Facile Strategy To Prepare Smart Coatings with Autonomous Self-Healing and Self-Reporting Functions.'' *ACS Appl. Mater. Interface.*, **12** (4) 4870–4877 (2020)
20. Attaei, M, Calado, LM, Taryba, MG, Morozov, Y, Shakoor, RA, Kahraman, R, Marques, AC, Fatima Montemor, M, ''Autonomous Self-Healing in Epoxy Coatings Provided by High Efficiency Isophorone Diisocyanate (IPDI) Microcapsules for Protection of Carbon Steel.'' *Prog. Org. Coat.,* **139** 105445 (2020)
21. Song, Y, Chen, K-F, Wang, J-J, Liu, Y, Qi, T, Li, GL, ''Synthesis of Polyurethane/Poly(Urea-Formaldehyde) Double-Shelled Microcapsules for Self-Healing Anticorrosion Coatings.'' *Chin. J. Polym. Sci.*, **38** (01) 45–56 (2020)
22. Gaaz, TS, Sulong, AB, Akhtar, MN, Kadhum, AAH, Mohamad, AB, Al-Amiery, AA, ''Properties and Applications of Polyvinyl Alcohol, Halloysite Nanotubes and Their Nanocomposites.'' *Molecules*, **20** (12) 22833–22847 (2015)
23. Kumar, A, Han, SS, ''PVA-Based Hydrogels for Tissue Engineering: A Review.'' *Int. J. Polym. Mater. Po.*, **66** (4) 159–182 (2017)
24. He, ZL, Jiang, S, An, N, Li, XD, Li, QF, Wang, JW, Zhao, YH, Kang, MQ, ''Self-Healing Isocyanate Microcapsules for Efficient Restoration of Fracture Damage of Polyurethane and Epoxy Resins.'' *J. Mater. Sci.*, **54** (11) 8262–8275 (2019)
25. He, Z, Jiang, S, Li, Q, Wang, J, Zhao, Y, Kang, M, ''Facile and Cost-Effective Synthesis of Isocyanate Microcapsules via Polyvinyl Alcohol-Mediated Interfacial Polymerization and Their Application in Self-Healing Materials.'' *Compos. Sci. Technol.*, **138** 15–23 (2017)
26. Zhang, F, Wang, YP, Yuan, L, Chai, CP, ''Synthesis of Acrylic Emulsion Containing High Hydroxyl Content.'' *J. Macromol. Sci. A.*, **A41** (1) 15–27 (2004)
27. Briscoe, B, Luckham, P, Zhu, S, ''The Effects of Hydrogen Bonding Upon the Viscosity of Aqueous Poly(Vinyl Alcohol) Solutions.'' *Polymer*, **41** (10) 3851–3860 (2000)
28. Ye, W-j, Lv, W-y, Mei, Q-q, Fu, H-k, Du, M, Zheng, Q, ''Influence of Hydrogen-bond on the Rheological Behavior of Poly (vinyl alcohol).'' *Acta. Polym. Sin.*, (10) 1216-1222 (2015)
29. Lee, H, Mensire, R, Cohen, RE, Rubner, MF, ''Strategies for Hydrogen Bonding Based Layer-by-Layer Assembly of Poly(Vinyl Alcohol) with Weak Polyacids.'' *Macromolecules*, **45** (1) 347–355 (2012)
30. Ma, WZ, Zhang, P, Zhao, B, Wang, SY, Zhong, J, Cao, Z, Liu, CL, Gong, FH, Matsuyama, H, ''Swelling Resistance and Mechanical Performance of Physical Crosslink-Based Poly(Vinyl Alcohol) Hydrogel Film with Various Molecular Weight.'' *J. Polym. Sci. Pol. Phys.*, **57** 1673–1683 (2019)
31. Wu, G, An, J, Sun, D, Tang, X, Xiang, Y, Yang, J, ''Robust Microcapsules with Polyurea/Silica Hybrid Shell for One-Part Self-Healing Anticorrosion Coatings.'' *J. Mater. Chem. A.*, **2** (30) 11614–11620 (2014)
32. Kim, S-R, Getachew, BA, Park, S-J, Kwon, O-S, Ryu, W-H, Taylor, AD, Bae, J, Kim, J-H, ''Toward Microcapsule-Embedded Self-Healing Membranes.'' *Environ. Sci. Tech. Let.*, **3** (5) 216–221 (2016)
33. Guo, ML, He, YY, Wang, JP, Zhang, XX, Li, W, ''Microencapsulation of Oil Soluble Polyaspartic Acid Ester and Isophorone Diisocyanate and Their Application in Self-Healing Anticorrosive Epoxy Resin.'' *J. Appl. Polym. Sci.*, **137** (12) 48478 (2020)